

Lung Microstructure Changes in a Rabbit after Elastase Instillation as Detected with Multiple Exchange Time XTC (MXTC)

I. Dregely¹, K. Ruppert², J. F. Mata², T. A. Altes², J. Ketel³, I. C. Ruset³, S. Ketel³, G. W. Miller², J. P. Mugler III², and F. W. Hersman^{1,3}

¹Physics, University of New Hampshire, Durham, NH, United States, ²Radiology, University of Virginia, Charlottesville, VA, United States, ³Xemed LLC, Durham, NH, United States

Introduction: Hyperpolarized xenon-129 MRI permits the collection of regional information about lung microstructure integrity by imaging the gas exchange of xenon between the alveoli and the surrounding septal walls. Xenon dissolved in tissue experiences a large chemical shift (~202 ppm in rabbits) relative to the gas phase resonance frequency. In xenon polarization transfer contrast (XTC) MRI the exchange of xenon is measured by monitoring the modulation of the gas phase magnetization due to its exchange with the dissolved phase, which is selectively saturated by 90° RF pulses [1,2]. We extend the XTC technique by acquiring 3D depolarization maps for multiple exchange times (MXTC). Since the xenon exchange is mapped for a range of delay times, the data can be fit to the xenon diffusion model such that tissue thickness and the relative tissue volume can be obtained. The purpose of this work is to evaluate the ability of 3D MXTC to detect global and regional changes in septal wall thickness and tissue-to-alveolar-volume ratio after the instillation of elastase into the lungs of a New Zealand rabbit.

Methods: A New Zealand rabbit was imaged with 3D MXTC before and three days after instillation of elastase. Three images (flip angles 2°, 2° and 4°) are acquired for the XTC technique. The xenon exchange contrast is generated between images two and three by selective saturation of dissolved phase xenon at 202 ppm with 1 ms 90° Gaussian RF pulses. Several saturation pulses are applied separated by a characteristic delay time to allow for xenon exchange between the gas and dissolved phases. Between image one and two the saturation pulses are applied at - 202 ppm and the ratio of the two images serves as a control to normalize the exchange ratio (images two and three) for T1 decay and RF effects [1,2]. Images were acquired using a 3D FLASH sequence with the following parameters: non-selective excitation with 500 μ s rectangular RF pulses; matrix size 12x28x32; TR/TE 6/3 ms; FOV 108 mm; receiver bandwidth 260 Hz/pixel. A xenon birdcage RF coil was used (IGC Medical Advances, Milwaukee, WI). All imaging was done on a 1.5 T commercial whole-body imager (Avanto, Siemens Medical Solutions). The New Zealand rabbit (~5 kg) was anesthetized with a mixture of Xylazine 5 mg/kg and Ketamine 50 mg/kg. For imaging the rabbit was intubated and ventilated immediately before the pulse sequence was started, using a syringe with 30 or 40 cc of isotopically enriched xenon gas (~87% xenon-129), hyperpolarized by a commercial prototype system to approximately 35% (Xemed LLC, Durham NH). After baseline imaging porcine elastase was instilled into the rabbit's lungs using a high-pressure microsprayer positioned just above the carina (PennCentury, Philadelphia, PA). The protocol was approved by our Institutional Animal Care and Use Committee. The 3D MXTC depolarization maps were fit to a simple diffusion model and parameter maps for the exchange time constant and maximum depolarization were obtained [1,3]:

$$f_D = \lambda \frac{V_t}{V_a} \cdot \left(1 - \frac{8}{\pi^2} \exp\left(-\frac{\tau}{\tau_c}\right) \right), \text{ where } f_D \text{ is the gas depolarization per } 90^\circ \text{ pulse, } \lambda \text{ is the Ostwald solubility, } \frac{V_t}{V_a} \text{ is the ratio of tissue and alveolar volume, } \tau \text{ is the delay time and } \tau_c \text{ is the exchange time constant.}$$

the delay time and τ_c is the exchange time constant.

Results: Figure 1 shows global depolarization values for xenon delay times between 5 and 200 ms. All imaging techniques involving the dissolved phase of xenon are sensitive to ventilation volume due to the decrease of tissue-to-alveolar-volume ratio with increasing lung inflation. If no changes to the lung parenchyma would have occurred due to the instillation of elastase, one would expect lower depolarization volumes for the 40 cc data obtained post elastase if compared to baseline obtained at a ventilation volume of 30 cc. However the depolarization measured post-elastase instillation is elevated at all delay times compared to the baseline. After independent fitting of each imaging voxel to the diffusion model, local xenon exchange can be characterized by a time constant and a maximum depolarization value. Figure 2 shows that these two fitting parameters are well correlated. If compared to baseline, post-elastase data appear spread more towards higher time constants and depolarization values. Assuming the diffusion constant for xenon in the parenchyma ($D = 3.3 \times 10^{-6} \text{ cm}^2/\text{s}$) does not change after elastase instillation, the tissue thickness can be calculated from the obtained time constant [1]: $L = \sqrt{D\tau_c\pi}$. The result is a mean septal wall thickness of 8.8 μm post-elastase, which is elevated compared to 8.0 μm at baseline. The mean ratio of tissue-to-alveolar volume can be determined from the maximum depolarization divided by the Ostwald solubility ($\lambda = 0.1$) and is also higher post-elastase (29%) compared to baseline (19%). Especially around the main airways, local tissue thickness is increased post-elastase instillation (arrow, Fig 3b) compared to baseline (Fig 3a). The same region has an increased tissue-to-alveolar volume ratio (post-elastase: Fig. 3d, baseline: Fig. 3c). These observations can be attributed to an initial severe inflammatory response that precedes subsequent tissue break down.

Conclusion: 3D MXTC detected elevated xenon exchange parameters in the lung parenchyma of a rabbit post-elastase instillation, indicating structural changes consistent with inflammation.

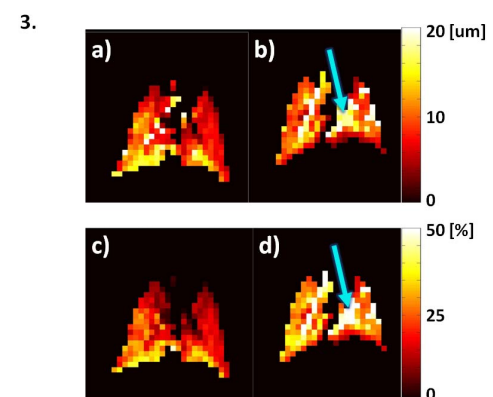
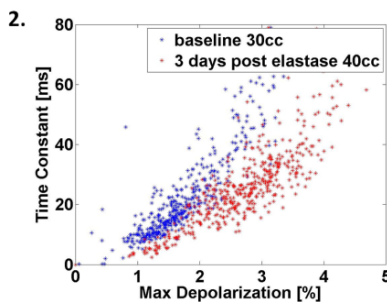
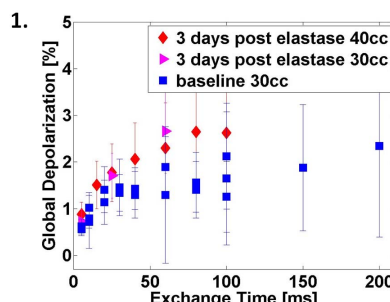


Figure 1: Global depolarization. **Figure 2:** Correlation of time constant and global depolarization. **Figure 3:** a) Septal wall thickness in μm at baseline and b) three days post elastase; c) tissue-to-alveolar volume ratio at baseline and d) post elastase.

References: [1] Ruppert K, Mata JF, Brookeman JR, Hagspiel KD, Driehuys B, Mugler III JP. MRM 2004; 51(4):676-87 [2] Patz, S.; Muradian, I.; Hrovat, M. I.; Ruset, I. C.; Topulos, G.; Covrig, S. D.; Frederick, E.; Hatabu, H.; Hersman, F. W. & Butler, J. P. Acad Rad 2008; 15(6):713-727 [3] Måansson, S.; Wolber, J.; Driehuys, B.; Wollmer, P. & Golman, K. MRM 2003; 50(6): 1170-1179.

Acknowledgements: Supported by NIH grants R42 HL082013, R01 EB003202 and R01 HL079077, the New Hampshire Innovation Research Center and Siemens Medical Solutions.